Copper Oxide-Antimony Oxide Entrapped Alginate Hydrogel as Efficient Catalyst for Selective Reduction of 2-Nitrophenol

Sher Bahadar Khan [1,2,*], Esraa M. Bakhsh [1], Kalsoom Akhtar [1], Tahseen Kamal [1,2], Yan Shen [3] and Abdullah M. Asiri [1,2]

[1] Chemistry Department, Faculty of Science, King Abdulaziz University, P.O. Box 80203, Jeddah 21589, Saudi Arabia; ibakhsh@kau.edu.sa (E.M.B.); kaskhan@kau.edu.sa (K.A.); tkkhan@kau.edu.sa (T.K.); aasiri2@kau.edu.sa (A.M.A.)
[2] Center of Excellence for Advanced Materials Research, King Abdulaziz University, P.O. Box 80203, Jeddah 21589, Saudi Arabia
[3] Wuhan National Laboratory for Optoelectronics, Huazhong University of Science and Technology, Luoyu Road 1037, Wuhan 430074, China; ciac_sheny@hust.edu.cn
* Correspondence: sbkhan@kau.edu.sa

Abstract: Copper oxide-antimony oxide (Cu_2O-Sb_2O_3) was prepared and entrapped inside Na-alginate hydrogel (Alg@Cu_2O-Sb_2O_3). The developed Alg@Cu_2O-Sb_2O_3 was used as catalytic reactor for the reduction of 4-nitrophenol (4-NP), 2-nitrophenol (2-NP), 2,6-dinitrophenol (2,6-DNP), methyl orange (MO), congo red (CR), acridine orange (AO), methylene blue (MB) and potassium ferricyanide ($K_3[Fe(CN)_6]$). Alg@Cu_2O-Sb_2O_3 was found to be selective and more efficient for the reduction of 2-NP among all the pollutants. Therefore, 2-NP was selected for a detailed study to optimize various parameters, e.g., the catalyst amount, reducing agent concentration, 2-NP concentration and recyclability. Alg@Cu_2O-Sb_2O_3 was found to be very stable and easily recyclable for the reduction of 2-NP. The Alg@Cu_2O-Sb_2O_3 nanocatalyst reduced 2-NP in 1.0 min, having a rate constant of $3.8187 \ min^{-1}$.

Keywords: Na-alginate; hydrogel wrapped copper oxide-antimony oxide; nitrophenols; dyes; potassium ferricyanide; catalytic reduction; water treatment; environmental applications

1. Introduction

Environmental pollution achieved worrying levels due to the continuous release and disposal of numerous pollutants into the environment and wastewater. Many of these pollutants are dyes and nitrophenols and are unsustainable in nature, which is of particularly great concern due to environmental regulations. These pollutants have high toxicity, hazardous nature, carcinogenicity, mutagenic nature, low biodegradability, and the fact that they are harmful and dangerous to living organisms [1,2]. Currently, dyes as well as phenols are believed to be tenacious, lethal, and dangerous contaminants coming from industrial wastewater [3,4]. These pollutants exist in the wastes of agrochemical, pharmaceutical, textile, and chemical industries because several industries are accountable for throwing out various pollutants into the ecosystem through wastewater streams. Consequently, the processes related to the disposal of the above-mentioned pollutants have foremost limitations, having a very slow removal proficiency, a poor elimination rate as well as being very costly and complex, which limits its applications [5,6]. Fortunately, researchers have focused a lot on detecting significant pollutants for different water bodies, but less work has been done on the removal or conversion of toxic pollutants [1,2]. Therefore, the efficient reduction and fast degradation of these pollutants is a central concern, considering its environmental and health hazards. One way to manage these pollutants from wastewater is by performing their reduction so as to produce less toxic or useful compounds.

Various techniques are utilized regarding the removal of lethal pollutants from contaminated water [7]. However, these processes are believed to not be very useful for the complete removal of dangerous pollutants, or they require a long time. Second, the high cost also reduces their importance. Thus, easy, uncomplicated, and cheap methods are required for managing polluted wastewater [3,8]. Catalytic reduction is considered an inexpensive and good technique as it is easy, fast, and proficient. Catalytic reduction involves a very low quantity of solvent, and the time required for removal is also very short [9–11]. In recent times, many efforts have been made to prepare new catalysts and enhance their catalytic performance and stability as well as their selectivity regarding water pollutants [12–14].

Nanomaterials have eccentric and numerous applications in relation to human health, which they confer significantly to medicine and the environment. Nanomaterials demonstrate a good ability as catalysts, which is hardly possible when considering conventional systems. Nanomaterials retain a distinct shape, small size, and remarkable surface activity [15–19]. Tin oxide possesses a good ability and many applications, but still, it requires reformation to enhance its catalytic properties [20–22]. When considering many techniques, doping is the one that is used to reveal excellent properties in various areas. Dopants works to increase the surface area and alter the structure, modifying the morphology, which leads to enhanced properties of nanomaterials [23,24].

Doped metal oxides are efficient catalysts, but their utilization in powder form has several drawbacks such as aggregation, regeneration of the catalyst, recyclability and leaching. Therefore, to solve these problems, a Cu_2O-Sb_2O_3 nanomaterial was wrapped inside Na-alginate hydrogel to prevent this agglomeration and to make the recycling of metal oxide nanocatalysts easy, which is the novelty of the current study. For the current study, Cu_2O-Sb_2O_3 nanomaterial was prepared and checked by FESEM, EDS, XRD and FTIR. Further Cu_2O-Sb_2O_3 was entrapped inside Na-alginate hydrogel. Alg@Cu_2O-Sb_2O_3 was initially tested for MO, CR, ArO, MB and $K_3[Fe(CN)_6]$, 4-NP, 2-NP and 2,6-DNP, and we explored the efficiency of the Alg@Cu_2O-Sb_2O_3 nanocatalyst for the reduction of these pollutants. The Alg@Cu_2O-Sb_2O_3 nanocatalyst achieved the greatest selectivity toward 2-NP, which underwent a reduction in 1.0 min, having a superior rate constant.

## 2. Experimental Section

2.1. Chemicals and Reagents

Sodium alginate $(NaC_6H_7O_6)_n$, copper nitrate, antimony chloride, $K_3[Fe(CN)_6]$ and $NaBH_4$ were obtained from Sigma Aldrich. 4-NP, 2-NP and 2,6-DNP were obtained from Fluka. MO, CR, ArO, and MB were obtained from Merck, Germany.

2.2. Preparation of Cu_2O-Sb_2O_3 and Alg@Cu_2O-Sb_2O_3

0.1 M solutions of antimony chloride and copper nitrate were initially prepared and then mixed. The mixed aqueous solution was stirred continuously, and then 0.1 M NH_4OH was added and the pH was increased to 10. The mixed solution was heated at 150.0 °C for 10 h in an oven using an autoclave. The product was then filtered. After filtration, the product was dried after washing it thoroughly and was calcined at 400.0 °C for 5 h. The preparation process of Alg@Cu_2O-Sb_2O_3 and its utilization has been shown in Scheme 1. Alg@Cu_2O-Sb_2O_3 composite hydrogel was readily prepared by dispersing 3, 5 and 10 mg of Cu_2O-Sb_2O_3 in 1 mL of Alg individually. After that, HCl solution was added to the mixed solution. Alg was turned into hydrogel by H^+ after adding HCl solution because of H^+ crosslinking Alg. Alg@Cu_2O-Sb_2O_3 was finally removed and washed by utilizing distilled water for the purpose of removing the unreacted H^+ present on the top surface of the hydrogel. The samples were examined by a field emission scanning electron microscope (FESEM, INSTRUMENT JSM-7600F, Japan), energy dispersive X-ray spectrometry (EDS, Oxford instruments Inc system), powder X-ray diffraction (XRD, ARL X'tra Thermo Scientific diffractometer), and a Fourier Transform Infrared spectrometer. The catalytic reduction was examined by a UV–Vis spectrometer (Evolution 300 by Thermo Scientific).
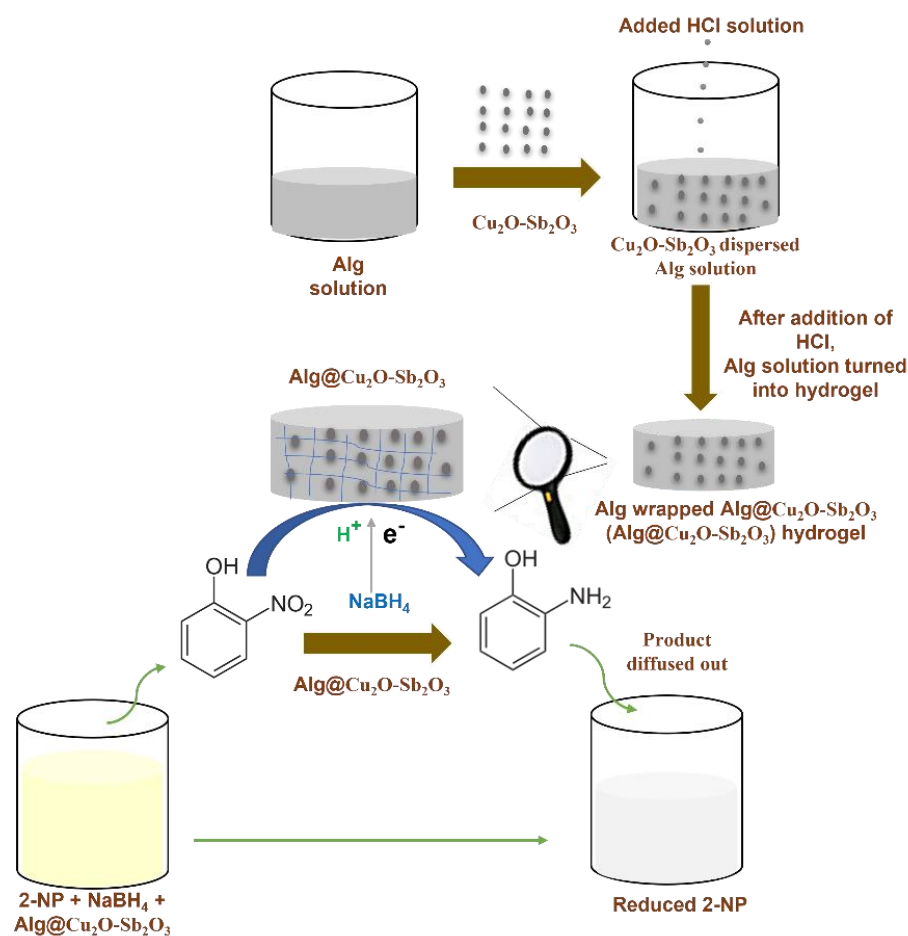
Scheme 1. Scheme of Alg@Cu$_2$O-Sb$_2$O$_3$ preparation and catalytic reduction of 2-NP.

2.3. Catalytic Reduction

At first, the Alg@Cu$_2$O-Sb$_2$O$_3$ hydrogel nanocatalyst was assessed with different dyes (CR (0.07 mM), MO (0.07 mM), ArO (0.07 mM), MB (0.07 mM)), K$_3$[Fe(CN)$_6$] (2.0 mM) and nitrophenols (4-NP (0.13 mM), 2-NP (0.13 mM) and 2,6-DNP (0.13 mM)). The catalytic reaction of the selected dyes, K$_3$[Fe(CN)$_6$] and nitrophenols was performed by Alg@Cu$_2$O-Sb$_2$O$_3$ catalyst in the presence of NaBH$_4$. 2.5 mL of pollutant solution was poured in a cuvette, and its UV spectrum was checked. 0.5 mL of NaBH$_4$ (0.1 M) was poured into it, followed by the addition of the Alg@Cu$_2$O-Sb$_2$O$_3$ hydrogel nanocatalyst to the reaction system, and then the UV–vis spectrum was measured with an interval of 1.0 min. Consequently, the catalytic reactions of CR, MO, ArO, MB, K$_3$[Fe(CN)$_6$], 4-NP, 2-NP and 2,6-DNP were analyzed by measuring the absorbance spectra at 490 nm, 460 nm, 465 nm, 658 nm, 415 nm, 400 nm, 413 nm and 428 nm, respectively, and the percent reduction (%R) was measured using Equation (1):

$$\%R = \frac{C_i - C_e}{C_i} \times 100 \qquad (1)$$

C_i = initial and C_e = final concentrations of pollutants.

3. Results and Discussion

3.1. Selection and Structure Interpretation of Cu$_2$O-Sb$_2$O$_3$ and Alg@Cu$_2$O-Sb$_2$O$_3$

In search of an efficient, stable, and economical catalyst, a huge number of materials have been investigated. Among different materials, nanomaterials containing metal oxides play a very important part as a catalyst. As a catalyst, metal oxides have displayed good catalytic activities when considering different reactions. Thus, it was thought that

doped metal oxides could be an excellent selection for the reduction reaction of pollutants. Consequently, Cu_2O-Sb_2O_3 and $Alg@Cu_2O$-Sb_2O_3 were prepared and tested in a reduction reaction of pollutants and discovered to be good catalysts because the $Alg@Cu_2O$-Sb_2O_3 nanocatalyst showed a superb catalytic activity in relation to the catalytic reduction reaction of pollutants. However, it was more efficient for the reactions involving the 2-NP reduction, and it was, therefore, suggested that the $Alg@Cu_2O$-Sb_2O_3 nanocatalyst was a better choice for the reduction of 2-NP. Additionally, the composition, chemical structure, and morphology of Cu_2O-Sb_2O_3 was evaluated by FESEM, EDS, XRD and ATR-FTIR. The wrapping of Cu_2O-Sb_2O_3 inside Alg was confirmed by XRD and ATR-FTIR.

FESEM was utilized to check the morphology of Cu_2O-Sb_2O_3, and the FESEM images are displayed in Figure 1. The surface morphology of Cu_2O-Sb_2O_3 was explicated by comparing both the low and high magnification images. The Cu_2O-Sb_2O_3 images indicate that it is grown like sheets, which combine to construct a flower-shaped structure. Thus, Cu_2O-Sb_2O_3 is grown in nanosheets, for which the sheet diameter was observed to be ~10 nm. The images clearly show that Cu_2O-Sb_2O_3 has a flower-shaped morphology, where the flower is made of aggregated nanosheets, collectively giving a flower structure.

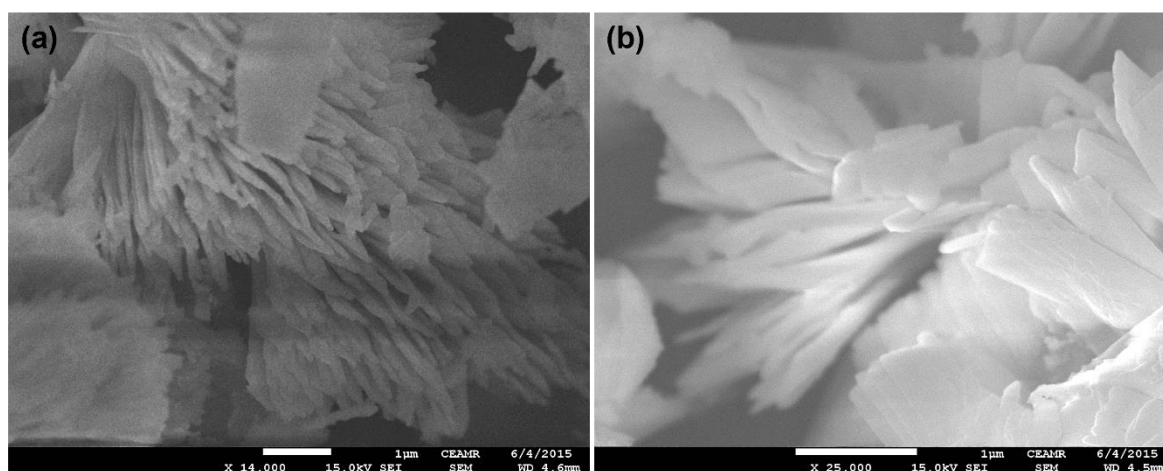**Figure 1.** FESEM images of Cu_2O-Sb_2O_3 at (**a**) ×14,000 and (**b**) ×25,000.

By using EDS, the compositional analysis of nanomaterial was examined, as shown in Figure 2. EDS displayed peaks related to antimony (Sb), copper (Cu) and oxygen (O), showing the existence of the corresponding elements and suggesting their existence in the prepared nanomaterial. EDS revealed 71 wt% of Sb and 3 wt% of Cu, indicating the growth of Cu_2O-doped Sb_2O_3. The lack of any extra peak in EDS suggested that the synthesized Cu_2O-Sb_2O_3 nanomaterial contained no impurity.

The XRD patterns of the prepared material clearly reveal peaks that correspond to the crystalline phase of Cu_2O and Sb_2O_3 (Figure 3a). Hence, the XRD patterns imply that the prepared material is comprised of Cu_2O and Sb_2O_3 phases. Cu_2O-Sb_2O_3 revealed diffraction peaks at 2θ = 20.0, 26.0, 29.3, 30.5, 33.0, 33.9, 36.4, 37.5, 40.3, 41.8, 45.8, 47.4, 49.1, 51.5, 53.2, 54.1, 56.3, 60.8, 63.2, 65.2, and 68.3°. The diffraction lines at 2θ = 30.5, 36.4 and 40.3°, which could be indexed to (110), (111), and (200), were assigned to Cu_2O [25,26]. All other peaks are well matched with the literature and could be assigned to the Sb_2O_3 phase. The intensities of the Cu_2O peaks are low in the XRD pattern, which might be due to the low quantity of Cu_2O phase present in Cu_2O-Sb_2O_3 when compared to the Sb_2O_3 phase. Therefore, the Sb_2O_3 diffraction peaks have significantly high intensities when compared to the Cu_2O peaks. The XRD pattern suggests the possible formation of a two-phase material composed of Cu_2O and Sb_2O_3 phases [24,27–29]. The $Alg@Cu_2O$-Sb_2O_3 hydrogel XRD only demonstrated the pattern of the amorphous material. This peak can be attributed to the amorphous phase of Alg. The $Alg@Cu_2O$-Sb_2O_3 pattern did not show any peak associated with the Cu_2O-Sb_2O_3 phase, the reason for this being either the presence of a lower quantity

of Cu_2O-Sb_2O_3 in Alg@Cu_2O-Sb_2O_3 or Cu_2O-Sb_2O_3 being entirely wrapped up inside the Alg hydrogel. Consequently, the XRD pattern of Alg@Cu_2O-Sb_2O_3 only displayed peaks associated with the Alg phase. Thus, the XRD pattern suggested that Cu_2O-Sb_2O_3 was ensnared inside the Alg hydrogel.
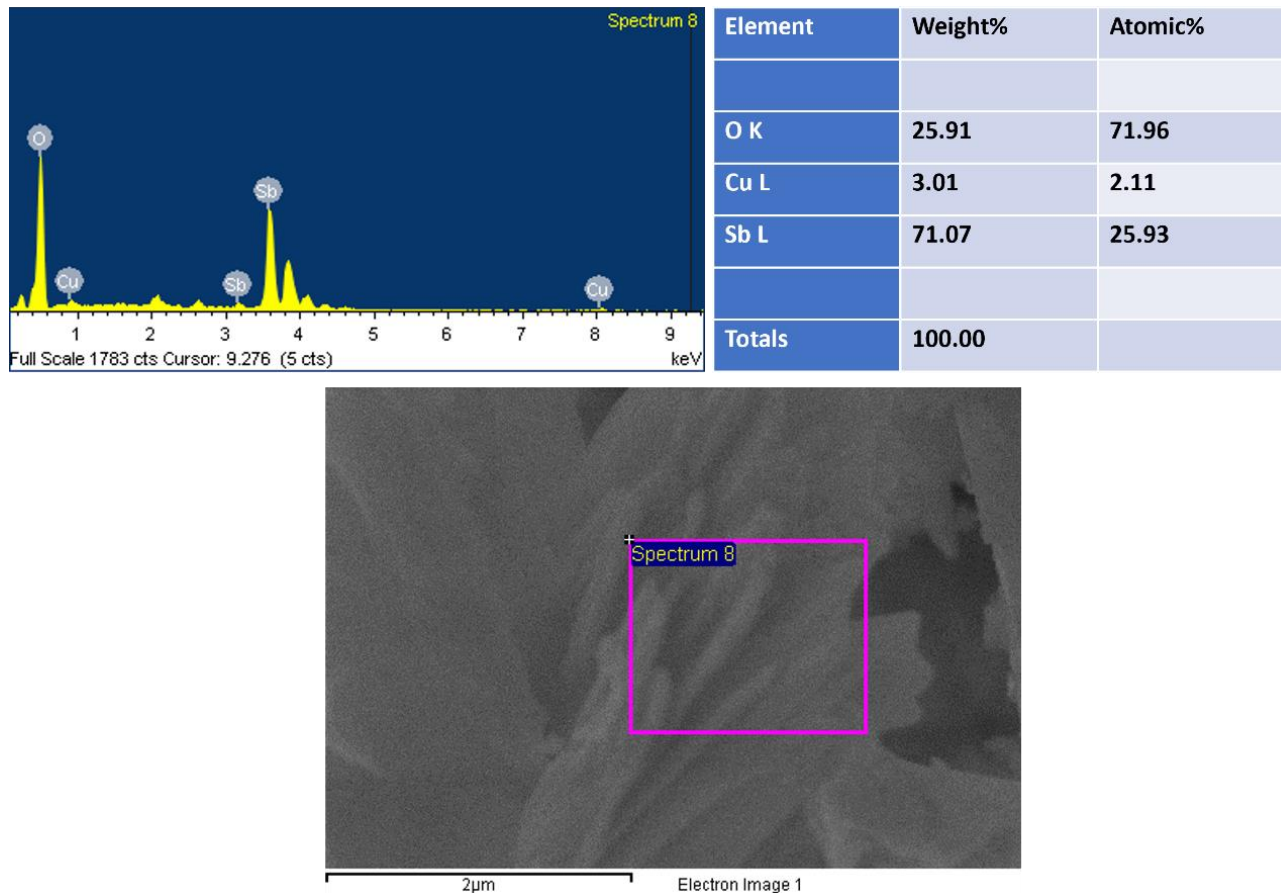
Element	Weight%	Atomic%
O K	25.91	71.96
Cu L	3.01	2.11
Sb L	71.07	25.93
Totals	100.00	

Figure 2. EDS of Cu_2O-Sb_2O_3.
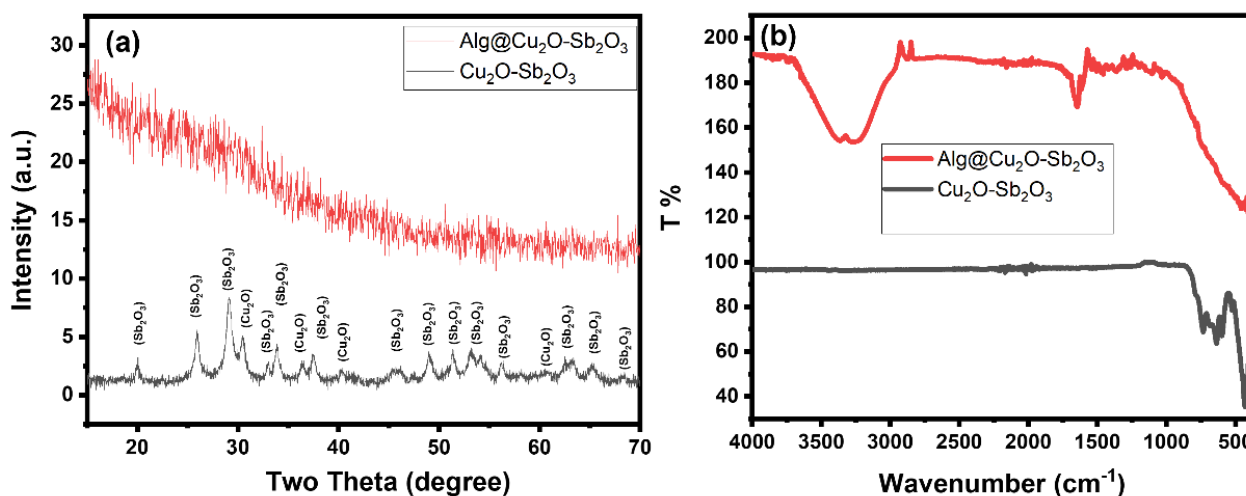
Figure 3. (**a**) XRD and (**b**) ATR-FTIR of Cu_2O-Sb_2O_3 and Alg@Cu_2O-Sb_2O_3 nanocatalysts.

The ATR-FTIR spectrum of Cu_2O-Sb_2O_3 indicated intense bands at 430, 590 and 631 cm^{-1} (Figure 3b). These bands indicate the growth of metal oxide (M=O stretching). The Alg@Cu_2O-Sb_2O_3 nanocatalyst also displayed a high and intense broad band in the same region (400~600 cm^{-1}), confirming the presence of Cu_2O-Sb_2O_3 [24,29]. The

Alg@Cu$_2$O-Sb$_2$O$_3$ nanocatalyst showed some additional bands at 1032, 1105, 1357, 1461, 1589, 1643, 1725, 2878, and 3200~3400, corresponding to Alg. The ATR-FTIR spectrum of Alg@Cu$_2$O-Sb$_2$O$_3$ indicated C–H and O–H bands at 2878 and 3268 cm^{-1}. The symmetric and asymmetric stretching vibration bands at 1461, 1643 and 1725 cm^{-1} were attributed to carboxylate salt ion and C=O. The C–O and C–C–H stretching vibration bands appeared at 1032, 1105 and 1357 cm^{-1}. The ATR-FTIR spectra suggest that Cu$_2$O-Sb$_2$O$_3$ and the Alg@Cu$_2$O-Sb$_2$O$_3$ nanocatalyst were prepared without any impurities.

3.2. Catalytic Activity of Alg@Cu$_2$O-Sb$_2$O$_3$

3.2.1. Reduction of Organic Dyes

Organic dyes are regarded as toxic pollutants, and consequently the prepared Alg@Cu$_2$O-Sb$_2$O$_3$ nanocatalyst was examined in order to evaluate the catalytic activity using NaBH$_4$. The Alg@Cu$_2$O-Sb$_2$O$_3$ nanocatalyst was applied for the reduction reaction of CR, MO, ArO and MB. Figure 4a–d exhibits the reduction of CR, MO, ArO and MB by NaBH$_4$ and Alg@Cu$_2$O-Sb$_2$O$_3$. The results indicate that Alg@Cu$_2$O-Sb$_2$O$_3$ reduced CR, MO, ArO and MB within 3.0–6.0 min (Figure 4a–d). The current findings suggest the reduction of the azo (-N=N-) group present in dye molecules through the transferring of electrons from BH$_4$$^-$ to Alg@Cu$_2$O-Sb$_2$O$_3$ and, further, through shifting electrons toward the acceptor dye molecules [30,31]. The conversion (%) was 97.14%, 97.86%, 50.59% and 97.38% for CR, MO, ArO and MB, respectively, within 4.0 min, 3.0 min, 6.0 min and 4.0 min (Figure 4e). The results suggested a high catalytic activity of Alg@Cu$_2$O-Sb$_2$O$_3$ toward the dyes reduction.

The pseudo-first-order equation was utilized to evaluate the reaction kinetics [32].

$$r = \frac{dc}{dt} = ln\frac{c_t}{c_0} = -k_{app}t \tag{2}$$

where r stands for the reactant rate; C is the reactant concentration; t stands for the time of reaction; k represents the reaction rate constant; C_t stands for the dyes concentration at time t; and C_0 stands for the dyes concentration at time 0.

The current study proves that the dyes reduction obeys pseudo-first-order kinetics. The rate constants were assessed as being 1.1929 min^{-1}, 1.4045 min^{-1}, 0.1131 min^{-1} and 0.9571 min^{-1} for CR, MO, ArO and MB, respectively. These high-rate constants suggest that there is a quick diffusion of BH$_4$$^-$ and dye molecules into Alg@Cu$_2$O-Sb$_2$O$_3$, where electron transfers take place from NaBH$_4$ to dye molecules and quickly diffuse out the product.

3.2.2. Reduction of K$_3$[Fe(CN)$_6$]

Alg@Cu$_2$O-Sb$_2$O$_3$ was tested in the reduction reaction of K$_3$[Fe(CN)$_6$] and NaBH$_4$. At first, the K$_3$[Fe(CN)$_6$] reduction was only performed by NaBH$_4$ without Alg@Cu$_2$O-Sb$_2$O$_3$. The K$_3$[Fe(CN)$_6$] reduction was very slow without Alg@Cu$_2$O-Sb$_2$O$_3$. Then, 10 mg of Alg@Cu$_2$O-Sb$_2$O$_3$ were placed into the mixture of NaBH$_4$ and K$_3$[Fe(CN)$_6$]. Using visual observation, it was noticed that K$_3$[Fe(CN)$_6$] bearing a yellow color faded immediately within few seconds and that within 3.0 min the absorbance band at 415 nm declined and disappeared, as demonstrated in Figure 5a. This indicates the reduction of Fe^{+3} to Fe^{+2} and hence the formation of [Fe(CN)$_6$]$^{-4}$ [33]. The conversion (%) was 97.98% for K$_3$[Fe(CN)$_6$] within 3.0 min (Figure 5b), and thus the current study indicated that a good reduction was attained by Alg@Cu$_2$O-Sb$_2$O$_3$; additionally, the results suggested a high catalytic property of Alg@Cu$_2$O-Sb$_2$O$_3$ toward the K$_3$[Fe(CN)$_6$] reduction. The kinetics of the K$_3$[Fe(CN)$_6$] reduction were analyzed by applying Equation (2), and the rate constant was assessed to be 1.3180 min^{-1}.
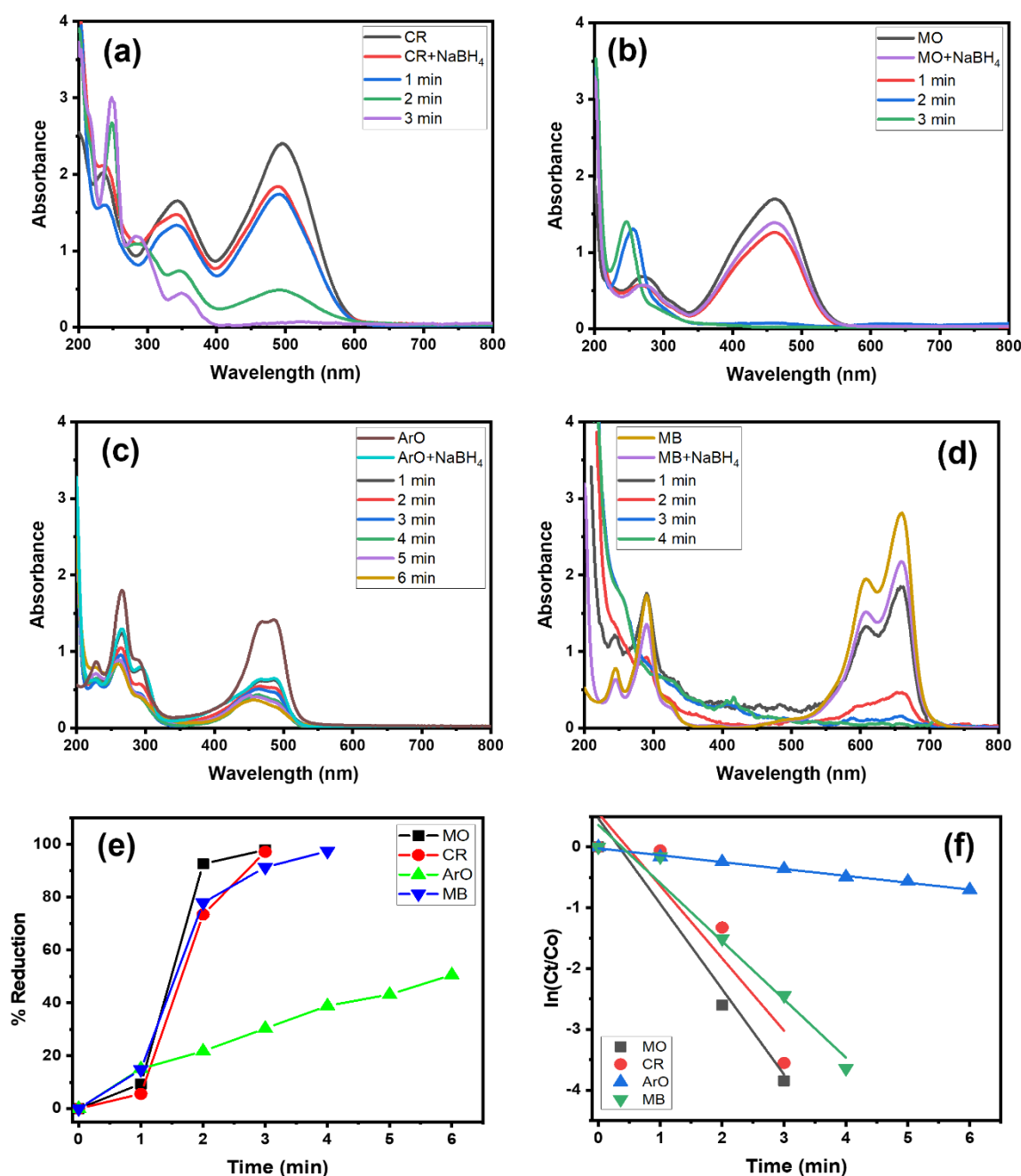
Figure 4. (**a–d**) UV–Vis spectra, (**e**) % reduction and (**f**) kinetics of CR, MO, ArO and MB reduction by NaBH$_4$ using 10 mg Alg@Cu$_2$O-Sb$_2$O$_3$ nanocatalyst.

3.2.3. Reduction of Nitrophenols

Alg@Cu$_2$O-Sb$_2$O$_3$ was also tested in the reduction reaction of 4-NP, 2-NP and 2,6-DNP with NaBH$_4$. Figure 6a reveals that 4-NP displayed an absorption peak at 317 nm. The addition of NaBH$_4$ caused a shift in absorption from 317 to 400 nm, signifying the formation of 4-nitrophenolate ions [24,34]. After adding Alg@Cu$_2$O-Sb$_2$O$_3$, the 4-nitrophenolate band at 400 nm gradually declined with time, which indicated that the –NO$_2$ group present in 4-NP got reduced to the –NH$_2$ group. The decline in the 4-nitrophenolate ion peak was faster for Alg@Cu$_2$O-Sb$_2$O$_3$, and the reaction was completed within 3.0 min. Similarly, Alg@Cu$_2$O-Sb$_2$O$_3$ was further analyzed in the reduction reaction of 2-NP and 2,6-DNP with NaBH$_4$ using UV–Vis spectrometry. Figure 6b,c illustrates that 2-NP and 2,6-DNP gave absorption peaks at 347 nm and 428 nm. Upon adding NaBH$_4$ solution, a change of color was noticed along with a shift in the absorption band from 347 nm to 413 nm for 2-NP, signifying

the existence of nitrophenolate ions [24,34]. Furthermore, upon adding Alg@Cu$_2$O-Sb$_2$O$_3$, the absorption peaks recorded at 413 nm and 428 nm declined, while, on the other hand, another absorption peak at 280 nm could be seen with an increasing trend in intensity. The results verify the conversion of nitrophenols to aminophenol by reducing NO$_2$ present in 2-NP and 2,6-DNP (Figure 6b,c). The 2-NP and 2,6-DNP reduction reactions were faster in the presence of Alg@Cu$_2$O-Sb$_2$O$_3$, and both reactions were completed within 1.0 min and 3.0 min, respectively. Alg@Cu$_2$O-Sb$_2$O$_3$ reduced more than 97% of 4-NP, 2-NP and 2,6-DNP in 3.0 min, 1.0 min and 3.0 min, respectively. Further, rate constants were obtained by applying Equation (2), and they were 1.3279 min^{-1}, 3.8187 min^{-1} and 1.2426 min^{-1} for 4-NP, 2-NP and 2,6-DNP, respectively. These results verify that the Alg@Cu$_2$O-Sb$_2$O$_3$ nanocatalyst is an effective catalyst, displaying more selectivity toward 2-NP.
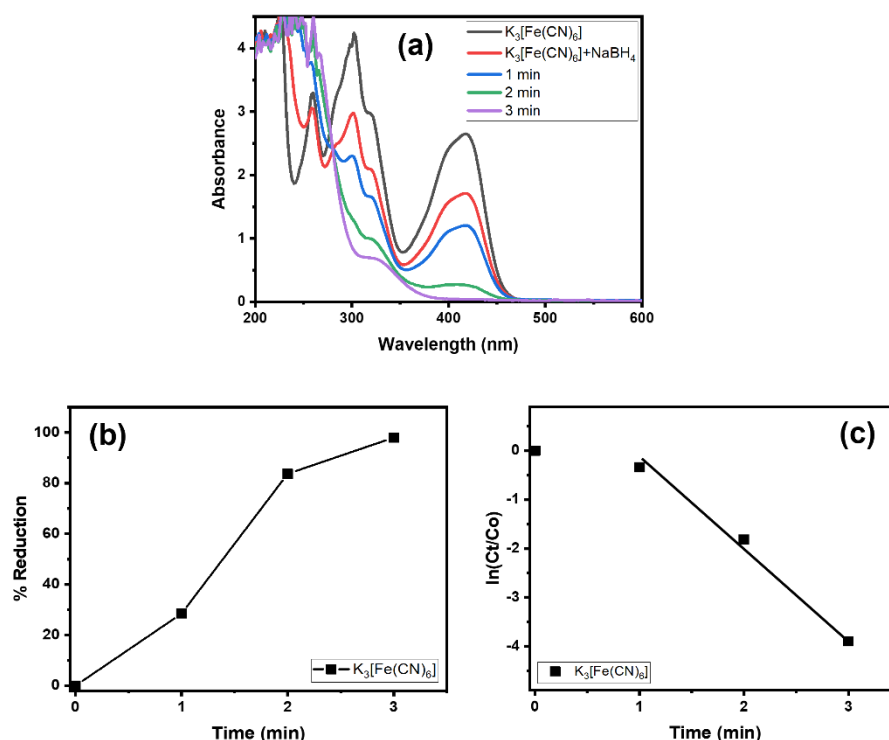

Figure 5. (**a**) UV–vis spectra, (**b**) % reduction and (**c**) kinetics of K$_3$[Fe(CN)$_6$] in the presence of NaBH$_4$ using 10 mg Alg@Cu$_2$O-Sb$_2$O$_3$ nanocatalyst.

Effect of Catalyst Amount

For a comprehensive study, we examined the impact of Alg@Cu$_2$O-Sb$_2$O$_3$ hydrogel and powder Cu$_2$O-Sb$_2$O$_3$ amounts on 2-NP reduction using NaBH$_4$ reducing agent. Hence, 3, 5 and 10 mg each of Cu$_2$O-Sb$_2$O$_3$ and Alg@Cu$_2$O-Sb$_2$O$_3$ nanocatalysts were added for the reduction of 2-NP to ascertain the impact of catalyst quantity (Figure 7). Figure 7g exhibits the graph of catalyst quantity vs. % reduction as well as the time consumed while maintaining constant amounts of NaBH$_4$ and 2-NP. The Alg@Cu$_2$O-Sb$_2$O$_3$ quantity plays a major role in speeding up the reaction and lowering the reaction time. 3 mg, 5 mg and 10 mg of Alg@Cu$_2$O-Sb$_2$O$_3$ reduced 2-NP in 8.0 min, 4.0 min and 1.0 min, respectively. Meanwhile, similar amounts of powder Cu$_2$O-Sb$_2$O$_3$ took 2.0 min and 1.0 min to reduce 2-NP. Thus, the role of Cu$_2$O-Sb$_2$O$_3$ and Alg@Cu$_2$O-Sb$_2$O$_3$ was evidently noticed, and hence, the Cu$_2$O-Sb$_2$O$_3$ and Alg@Cu$_2$O-Sb$_2$O$_3$ quantity plays a substantial role in the rate of 2-NP reduction. Therefore, Cu$_2$O-Sb$_2$O$_3$ is very effective, but powder Cu$_2$O-Sb$_2$O$_3$ has limitations, i.e., it is difficult to separate from the reaction in comparison with the present hydrogel. The powder catalyst has the drawback that it cannot be collected and separated from reaction media in order to recycle it. Hence, a requirement for a good catalyst would

be to remove or reduce these concerns. Consequently, Cu_2O-Sb_2O_3 was packed in hydrogel for the purpose of handling and surmounting all the above-mentioned concerns.
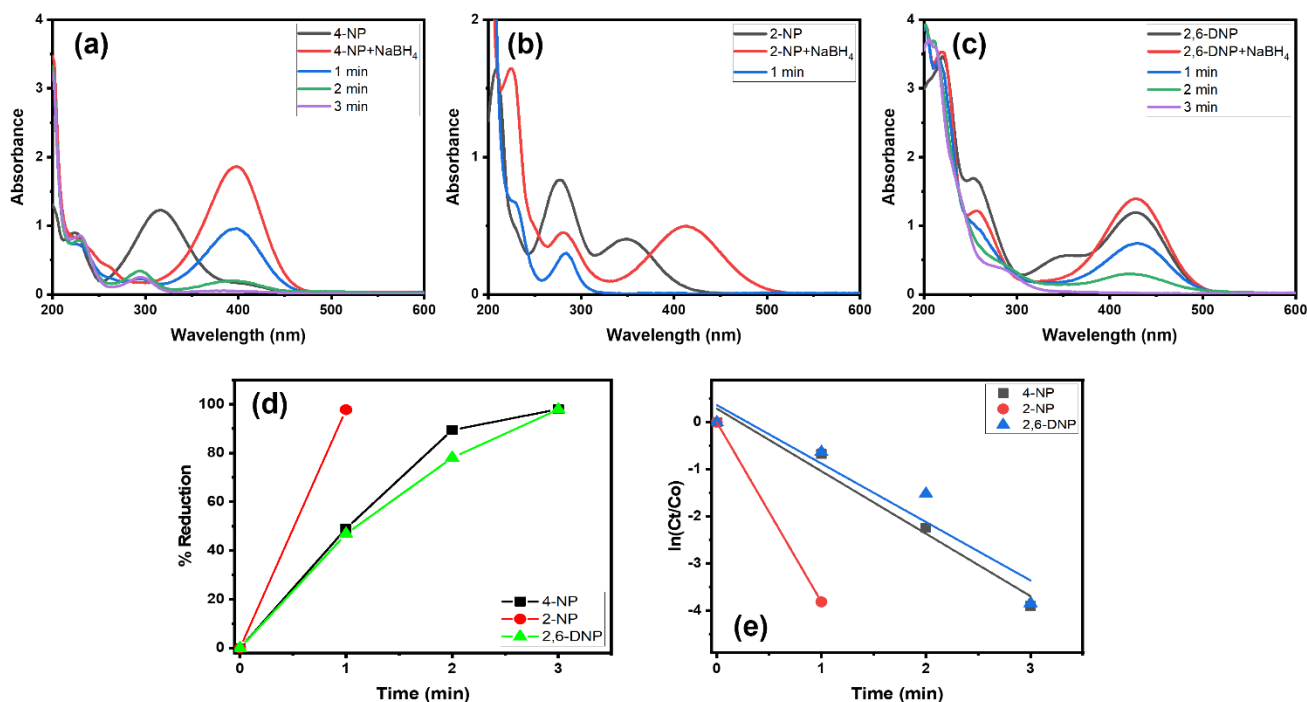

Figure 6. (**a**–**c**) UV–Vis spectra, (**d**) % reduction and (**e**) kinetics of 4-NP, 2-NP and 2,6-DNP in the presence of $NaBH_4$ using 10 mg Alg@Cu_2O-Sb_2O_3 nanocatalyst.

Effect of $NaBH_4$ Concentration

The impact of the $NaBH_4$ amount was assessed in the 2-NP reduction using the Alg@Cu_2O-Sb_2O_3 nanocatalyst. To scrutinize various quantities of $NaBH_4$, 0.3, 0.5 and 0.7 mL of 0.1 M $NaBH_4$ were utilized with 5 mg of Alg@Cu_2O-Sb_2O_3. Figure 8d shows the % reduction against the time plot. 2-NP got reduced up to 95.40%, 96.36% and 96.43% using 0.3, 0.5 and 0.7 mL of 0.1 M $NaBH_4$ solution. Further, the reaction rates calculated in the current study were 0.4649 min^{-1}, 0.7937 min^{-1} and 1.0599 min^{-1}.

Effect of 2-NP Concentration

Moreover, we examined the catalytic behavior of Alg@Cu_2O-Sb_2O_3 in the reduction of different concentrations of 2-NP in the presence of $NaBH_4$ (Figure 9). Consequently, various amounts of 2-NP solution (0.056, 0.074 and 0.093 mM) were used to ascertain the catalytic ability of Alg@Cu_2O-Sb_2O_3. Alg@Cu_2O-Sb_2O_3 reduced 92.49%, 97.49% and 97.36% of 0.056, 0.074 and 0.093 mM 2-NP in 2.0, 3.0 and 4.0 min with reaction rates of 1.2946 min^{-1}, 1.1388 min^{-1} and 0.7939 min^{-1}. Thus, a lower concentration of 2-NP reduces more efficiently when compared to high-concentrated 2-NP.
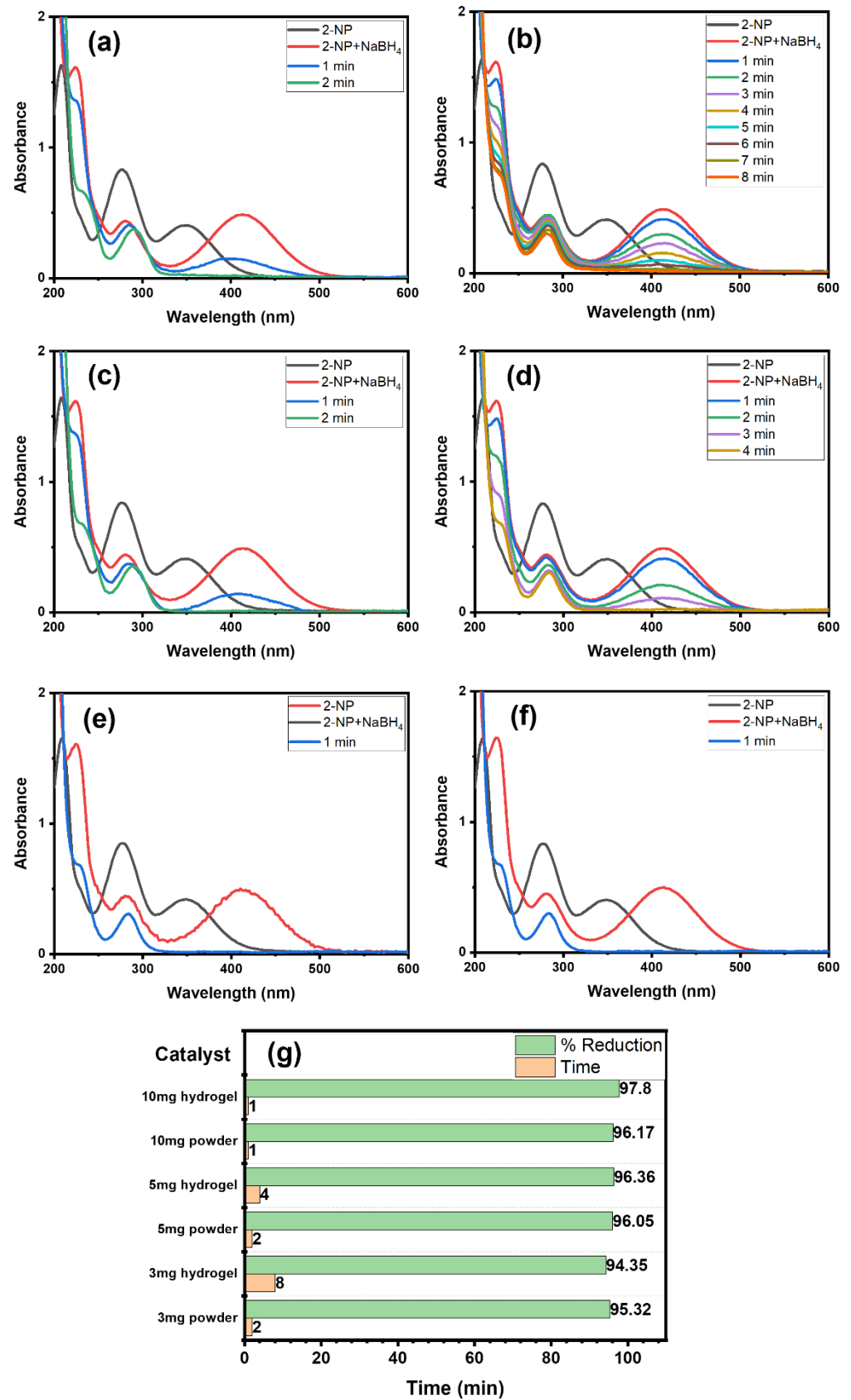
Figure 7. UV–Vis spectra: (**a**) 3 mg Cu$_2$O-Sb$_2$O$_3$, (**b**) 3 mg Alg@Cu$_2$O-Sb$_2$O$_3$, (**c**) 5 mg Cu$_2$O-Sb$_2$O$_3$, (**d**) 5 mg Alg@Cu$_2$O-Sb$_2$O$_3$, (**e**) 10 mg Cu$_2$O-Sb$_2$O$_3$, and (**f**) 10 mg Alg@Cu$_2$O-Sb$_2$O$_3$, (**g**) % reduction with the required time for 2-NP reduction in the presence of NaBH$_4$.
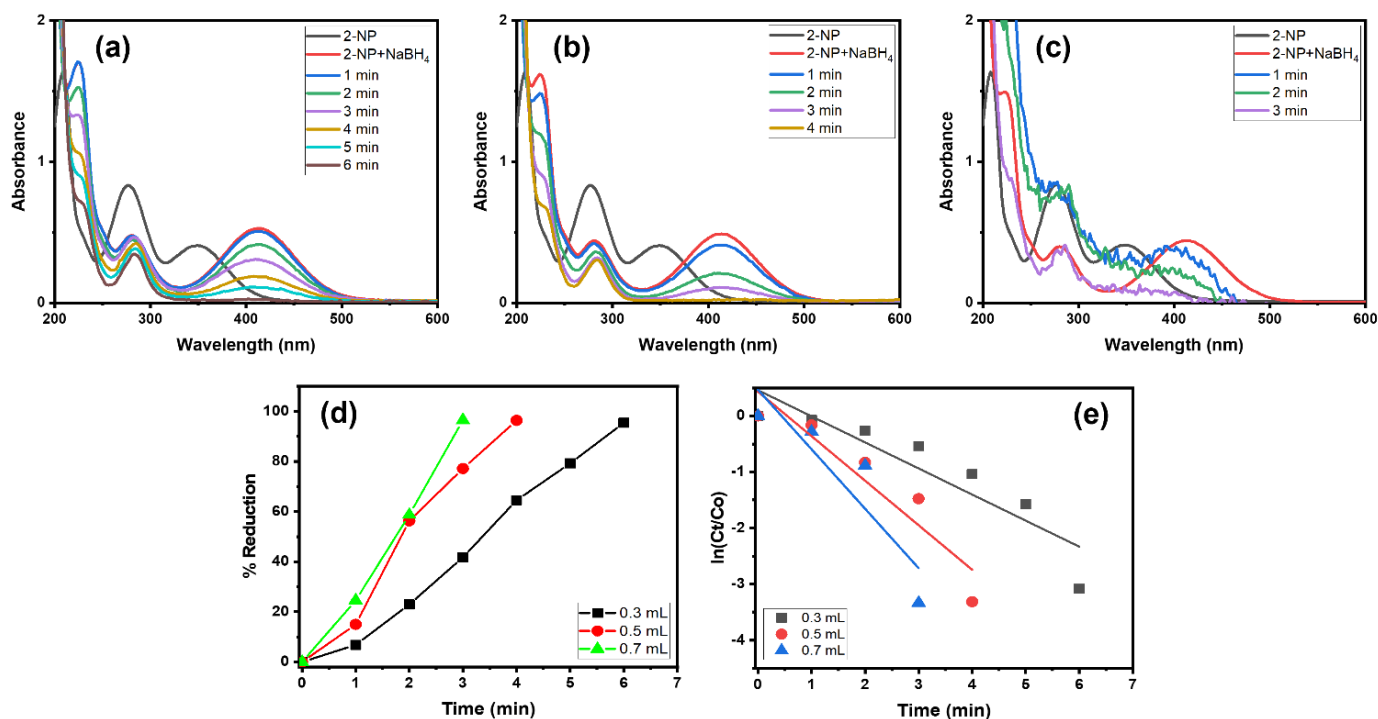
Figure 8. UV–Vis spectra in the presence of (**a**) 0.3 mL, (**b**) 0.5 mL and (**c**) 0.7 mL NaBH$_4$, (**d**) % reduction and (**e**) kinetics of 2-NP using 5 mg Alg@Cu$_2$O-Sb$_2$O$_3$ nanocatalyst.
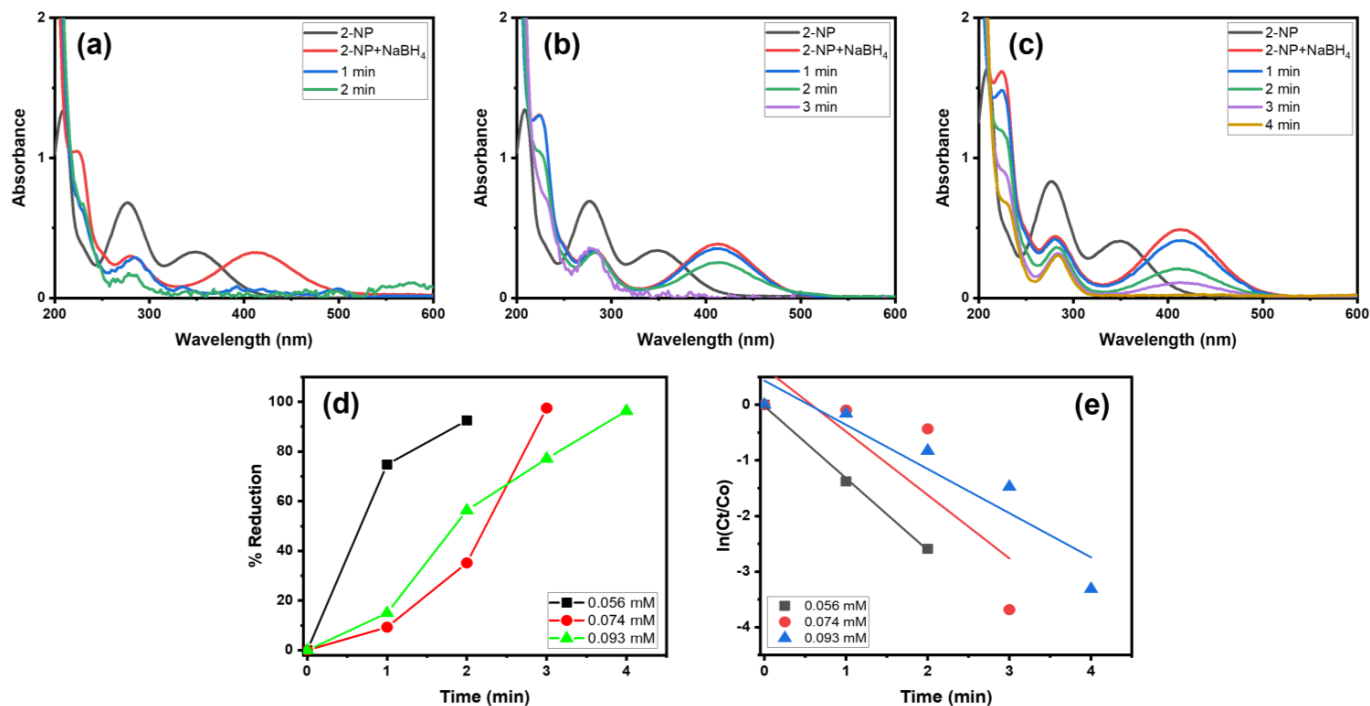

Figure 9. UV–Vis spectra of 2-NP reduction: (**a**) 0.065 mM, (**b**) 0.074 mM, and (**c**) 0.093 mM, (**d**) % reduction and (**e**) kinetics using 5 mg Alg@Cu$_2$O-Sb$_2$O$_3$ and 0.5 mL NaBH$_4$.

Recyclability of Alg@Cu$_2$O-Sb$_2$O$_3$

Catalyst consistency and recovery are important from an environmental and cost-based point of view [13,35]. Therefore, we checked the recyclability property of the Alg@Cu$_2$O-Sb$_2$O$_3$ nanocatalyst (Figure 10). We have analyzed the Alg@Cu$_2$O-Sb$_2$O$_3$ nanocatalyst four times for an easy removal of the product by means of just removing the hydrogel. Figure 10d specifies the time utilized for the reduction reaction of 2-NP in every cycle

with the same Alg@Cu_2O-Sb_2O_3 nanocatalyst, which suggests the stability as well as the recyclability property of Alg@Cu_2O-Sb_2O_3. Alg@Cu_2O-Sb_2O_3 efficiently reduced 2-NP in 4.0 min until the 3rd cycle, which suggests that Alg@Cu_2O-Sb_2O_3 can be used numerous times with no loss in catalytic activity. The results were compared with the literature [36–40], and it was fount that Alg@Cu_2O-Sb_2O_3 is an efficient catalyst that can be used several times. This indicate that nanocomposite can play important role as a catalyst since nanocomposites have shown an enormous range of applications in different sectors [41–43].
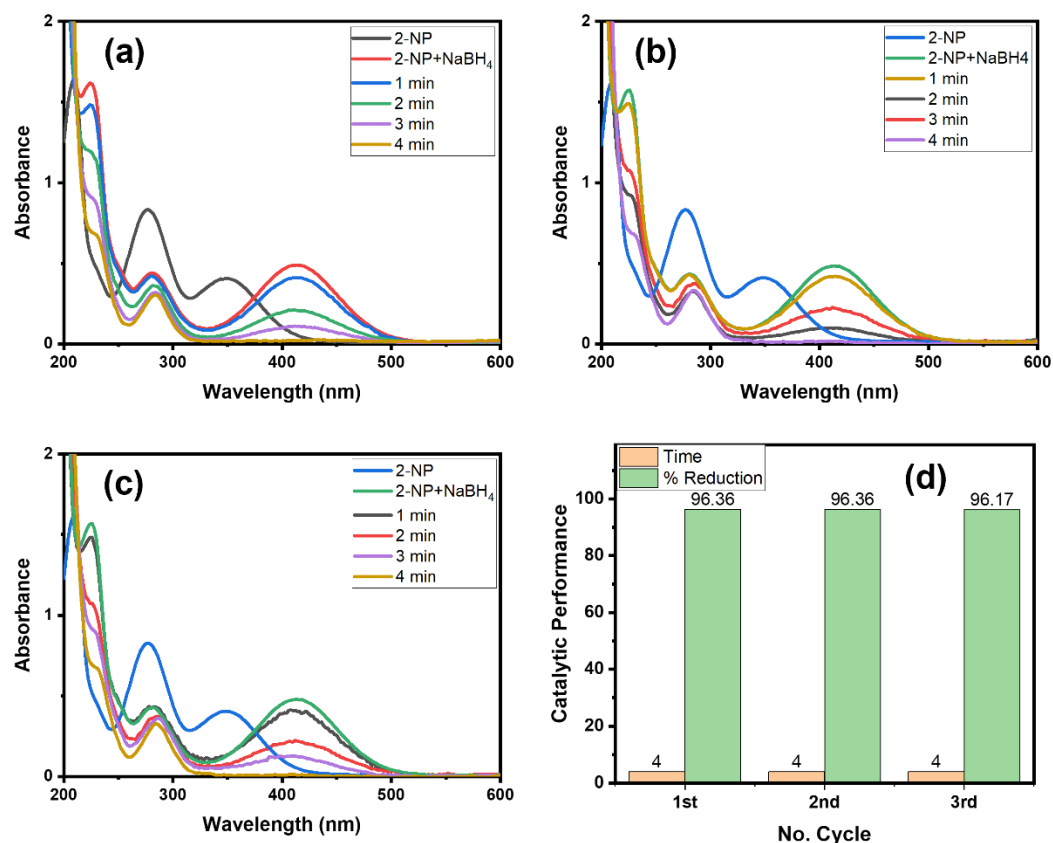

Figure 10. UV–Vis spectra for the reduction of 2-NP: (**a**) 1st cycle, (**b**) 2nd cycle, (**c**) 3rd cycle, and (**d**) comparative reduction time and % reduction in terms of recyclability using 5 mg Alg@Cu_2O-Sb_2O_3 in 2 mL 2-NP and 0.5 mL $NaBH_4$.

4. Conclusions

Cu_2O-Sb_2O_3 nanoparticles were prepared and placed inside the Alg hydrogel. Both Cu_2O-Sb_2O_3 and Alg@Cu_2O-Sb_2O_3 nanocatalysts were excellent catalysts for the selective reduction reaction of 2-NP. The influence of various parameters on the 2-NP reduction using Alg@Cu_2O-Sb_2O_3 showed that increasing the catalyst and $NaBH_4$ amounts and decreasing the 2-NP concentration preceded a greater catalytic efficiency. The rate constant when utilizing 10 mg Alg@Cu_2O-Sb_2O_3 was calculated as being 3.8187 min^{-1} for the 2-NP reduction. Lastly, Alg@Cu_2O-Sb_2O_3 maintained a greater activity after recyclability assessments.

Author Contributions: Conceptualization, S.B.K. and Y.S.; methodology, S.B.K.; software, T.K.; validation, T.K., Y.S. and A.M.A.; formal analysis, K.A.; investigation, E.M.B.; resources, A.M.A.; data curation, E.M.B.; writing—original draft preparation, K.A.; writing—review and editing, E.M.B.; visualization, T.K.; supervision, A.M.A.; project administration, K.A.; funding acquisition, S.B.K. All authors have read and agreed to the published version of the manuscript.

Institutional Review Board Statement: Not applicable.

Informed Consent Statement: Not applicable.

References

1. Dudgeon, D.; Arthington, A.H.; Gessner, M.O.; Kawabata, Z.-I.; Knowler, D.J.; Lévêque, C.; Naiman, R.J.; Prieur-Richard, A.-H.; Soto, D.; Stiassny, M.L.J.; et al. Freshwater biodiversity: Importance, threats, status and conservation challenges. *Biol. Rev.* **2006**, *81*, 163–182. [CrossRef] [PubMed]
2. Horton, A.A.; Walton, A.; Spurgeon, D.J.; Lahive, E.; Svendsen, C. Microplastics in freshwater and terrestrial environments: Evaluating the current understanding to identify the knowledge gaps and future research priorities. *Sci. Total Environ.* **2017**, *586*, 127–141. [CrossRef]
3. Rasalingam, S.; Peng, R.; Koodali, R.T. Removal of Hazardous Pollutants from Wastewaters: Applications of TiO_2-SiO_2 mixed oxide materials. *J. Nanomater.* **2014**, *2014*, 617405. [CrossRef]
4. Khan, S.A.; Bakhsh, E.M.; Asiri, A.M.; Khan, S.B. Chitosan coated NiAl layered double hydroxide microsphere templated zero-valent metal NPs for environmental remediation. *J. Clean. Prod.* **2021**, *285*, 124830. [CrossRef]
5. Villegas, L.G.C.; Mashhadi, N.; Chen, M.; Mukherjee, D.; Taylor, K.E.; Biswas, N. A short review of techniques for phenol removal from wastewater. *Curr. Pollut. Rep.* **2016**, *2*, 157–167. [CrossRef]
6. Maslamani, N.; Khan, S.B.; Danish, E.Y.; Bakhsh, E.M.; Zakeeruddin, S.M.; Asiri, A.M. Super adsorption performance of carboxymethyl cellulose/copper oxide-nickel oxide nanocomposite toward the removal of organic and inorganic pollutants. *Environ. Sci. Pollut. Res.* **2021**, *28*, 38476–38496. [CrossRef]
7. Tanikkul, S.; Jakmunee, J.; Lapanantnoppakhun, S.; Rayanakorn, M.; Sooksamiti, P.; Synovec, R.E.; Christian, G.D.; Grudpan, K. Flow injection invalve mini-column pretreatment combined with ion chromatography for cadmium, lead and zinc determination. *Talanta* **2004**, *64*, 1241–1246. [CrossRef] [PubMed]
8. Raza, W.; Lee, J.; Raza, N.; Luo, Y.; Kim, K.-H.; Yang, J. Removal of phenolic compounds from industrial waste water based on membrane-based technologies. *J. Ind. Eng. Chem.* **2019**, *71*, 118. [CrossRef]
9. Zhu, J.; Zhang, X.; Qin, Z.; Zhang, L.; Ye, Y.; Cao, M.; Gao, L.; Jiao, T. Preparation of PdNPs doped chitosan-based composite hydrogels as highly efficient catalysts for reduction of 4-nitrophenol. *Colloids Surf. A Physicochem. Eng. Asp.* **2021**, *611*, 125889. [CrossRef]
10. Xie, R.; Wei, T.; Bai, S.; Wang, Z.; Chai, F.; Chen, L.; Zang, S. The synthesis and catalytic activity of bimetallic CuAg nanoparticles and their magnetic hybrid composite materials. *New J. Chem.* **2020**, *44*, 9684–9690. [CrossRef]
11. Danish, E.Y.; Bakhsh, E.M.; Akhtar, K. Design of chitosan nanocomposite hydrogel for sensitive detection and removal of organic pollutants. *Int. J. Biol. Macromol.* **2020**, *159*, 276–286. [CrossRef]
12. Khan, S.B.; Ahmad, S.; Kamal, T.; Asiri, A.M.; Bakhsh, E.M. Metal nanoparticles decorated sodium alginate-carbon nitride composite beads as effective catalyst for the reduction of organic pollutants. *Int. J. Biol. Macromol.* **2020**, *164*, 1087–1098. [CrossRef]
13. Akhtar, K.; Ali, F.; Sohni, S.; Kamal, T.; Asiri, A.M.; Bakhsh, E.M.; Khan, S.B. Lignocellulosic biomass supported metal nanoparticles for the catalytic reduction of organic pollutants. *Environ. Sci. Pollut. Res.* **2020**, *27*, 823–836. [CrossRef]
14. Naseem, K.; Farooqi, Z.H.; Begum, R.; Irfan, A. Removal of Congo red dye from aqueous medium by its catalytic reduction using sodium borohydride in the presence of various inorganic nano-catalysts: A review. *J. Clean. Prod.* **2018**, *187*, 296–307. [CrossRef]
15. Bakhsh, E.M.; Khan, S.B.; Asiri, A.M.; Shah, A. Zn/Fe nanocomposite based efficient electrochemical sensor for the simultaneous detection of metal ions. *Phys. E Low-Dimens. Syst. Nanostruct.* **2021**, *130*, 114671. [CrossRef]
16. Khan, S.B.; Khan, M.S.J.; Kamal, T.; Asiri, A.M.; Bakhsh, E.M. Polymer supported metallic nanoparticles as a solid catalyst for the removal of organic pollutants. *Cellulose* **2020**, *27*, 5907–5921. [CrossRef]
17. Jang, E.S.; Khan, S.B.; Seo, J.; Nam, Y.H.; Choi, W.J.; Akhtar, K.; Han, H. Synthesis and characterization of novel UV-curable polyurethane-clay nanohybrid: Influence of organically modified layered silicates on the properties of polyurethane. *Prog. Org. Coat.* **2011**, *71*, 36–42. [CrossRef]
18. Gul, S.; Rehan, Z.A.; Khan, S.A.; Akhtar, K.; Khan, M.A.; Khan, M.I.; Rashid, M.I.; Asiri, A.M.; Khan, S.B. Antibacterial PES-CA-Ag_2O nanocomposite supported Cu nanoparticles membrane toward ultrafiltration, BSA rejection and reduction of nitrophenol. *J. Mol. Liq.* **2017**, *230*, 616–624. [CrossRef]
19. Lee, Y.; Kim, D.; Seo, J.; Han, H.; Khan, S.B. Preparation and characterization of poly(propylene carbonate)/exfoliated graphite nanocomposite films with improved thermal stability, mechanical properties and barrier properties. *Polym. Int.* **2013**, *62*, 1386–1394. [CrossRef]
20. Bakhsh, E.M.; Akhtar, K.; Fagieh, T.M.; Khan, S.B.; Asiri, A.M. Development of alginate@tin oxide-cobalt oxide nanocomposite based catalyst for the treatment of wastewater. *Int. J. Biol. Macromol.* **2021**, *187*, 386–398. [CrossRef] [PubMed]
21. Khan, S.B.; Kamal, T.; Asiri, A.M.; Bakhsh, E.M. Iron doped nanocomposites based efficient catalyst for hydrogen production and reduction of organic pollutant. *Colloids Surf. A Physicochem. Eng. Asp.* **2021**, *608*, 125502. [CrossRef]

22. Khan, S.B.; Khan, M.S.J.; Akhtar, K.; Bakhsh, E.M.; Kamal, T.; Asiri, A.M.; Shen, Y. Design of efficient solar photocatalytic system for hydrogen production and degradation of environmental pollutant. *J. Mater. Res. Technol.* **2021**, *14*, 2497–2512. [CrossRef]

23. Danish, M.S.; Bhattacharya, A.; Stepanova, D.; Mikhaylov, A.; Grilli, M.L.; Khosravy, M.; Senjyu, T. A systematic review of metal oxide applications for energy and environmental sustainability. *Metals* **2020**, *10*, 1604. [CrossRef]

24. Khan, S.B.; Akhtar, K.; Bakhsh, E.M.; Asiri, A.M. Electrochemical detection and catalytic removal of 4-nitrophenol using CeO_2-Cu_2O and CeO_2-Cu_2O/CH nanocomposites. *Appl. Surf. Sci.* **2019**, *492*, 726–735. [CrossRef]

25. Vázquez-López, A.; Yaseen, A.; Maestre, D.; Ramírez-Castellanos, J.; Marstein, E.S.; Karazhanov, S.Z.; Cremades, A. Synergetic improvement of stability and conductivity of hybrid composites formed by PEDOT:PSS and SnO nanoparticles. *Molecules* **2020**, *25*, 695. [CrossRef] [PubMed]

26. Janardhan, E.; Reddy, M.M.; Reddy, P.V.; Reddy, M.J. Synthesis of SnO nanoparticles—A hydrothermal approach. *World J. Nano Sci. Eng.* **2018**, *8*, 33–37. [CrossRef]

27. Marwani, H.M.; Bakhsh, E.M.; Khan, S.B.; Danish, E.Y.; Asiri, A.M. Cerium oxide-cadmium oxide nanomaterial as efficient extractant for yttrium ions. *J. Mol. Liq.* **2018**, *269*, 252–259. [CrossRef]

28. Chen, X.; Wang, X.; An, C.; Liu, J.; Qian, Y. Synthesis of Sb_2O_3 nanorods under hydrothermal conditions. *Mater. Res. Bull.* **2005**, *40*, 469–474. [CrossRef]

29. Liu, Y.; Wang, H.; Yang, K.; Yang, Y.; Ma, J.; Pan, K.; Wang, G.; Ren, F.; Pang, H. Enhanced electrochemical performance of Sb_2O_3 as an anode for lithium-ion batteries by a stable cross-linked binder. *Appl. Sci.* **2019**, *9*, 2677. [CrossRef]

30. Khan, S.A.; Khan, S.B.; Farooq, A.; Asiri, A.M. A facile synthesis of CuAg nanoparticles on highly porous ZnO/carbon black-cellulose acetate sheets for nitroarene and azo dyes reduction/degradation. *Int. J. Biol. Macromol.* **2019**, *130*, 288–299. [CrossRef]

31. Wang, W.; Wang, F.; Kang, Y.; Wang, A. Facile self-assembly of Au nanoparticles on a magnetic attapulgite/Fe_3O_4 composite for fast catalytic decoloration of dye. *RSC Adv.* **2013**, *3*, 11515–11520. [CrossRef]

32. Khan, F.U.; Asimullah; Khan, S.B.; Kamal, T.; Asiri, A.M.; Khan, I.U.; Akhtar, K. Novel combination of zero-valent Cu and Ag nanoparticles @ cellulose acetate nanocomposite for the reduction of 4-nitro phenol. *Int. J. Biol. Macromol.* **2017**, *102*, 868–877. [CrossRef] [PubMed]

33. Veerakumar, P.; Salamalai, K.; Thanasekaran, P.; Lin, K.-C. Simple preparation of porous carbon-supported ruthenium: Propitious catalytic activity in the reduction of ferrocyanate(III) and a cationic dye. *ACS Omega* **2018**, *3*, 12609–12621. [CrossRef]

34. Bae, S.; Gim, S.; Kim, H.; Hanna, K. Effect of $NaBH_4$ on properties of nanoscale zero-valent iron and its catalytic activity for reduction of p-nitrophenol. *Appl. Catal. B Environ.* **2016**, *182*, 541–549. [CrossRef]

35. Khan, S.A.; Khan, N.; Irum, U.; Farooq, A.; Asiri, A.M.; Bakhsh, E.M.; Khan, S.B. Cellulose acetate-Ce/Zr@Cu^0 catalyst for the degradation of organic pollutant. *Int. J. Biol. Macromol.* **2020**, *153*, 806–816. [CrossRef] [PubMed]

36. Sahiner, N.; Ozay, H.; Ozay, O.; Aktas, N. New catalytic route: Hydrogels as templates and reactors for in situ Ni nanoparticle synthesis and usage in the reduction of 2- and 4-nitrophenols. *Appl. Catal. A Gen.* **2010**, *385*, 201–207. [CrossRef]

37. Korobeinyk, A.V.; Whitby, R.D.L.; Mikhalovsky, S.V.; Inglezakis, V.J. In situ production of high purity noble metal nanoparticles on fumed silica and catalytic activity towards 2-nitrophenol reduction. *J. Phys. Chem. Solids* **2019**, *127*, 28–34. [CrossRef]

38. Ismail, M.; Khan, M.I.; Khan, S.B.; Akhtar, K.; Khan, M.A.; Asiri, A.M. Catalytic reduction of picric acid, nitrophenols and organic azo dyes via green synthesized plant supported Ag nanoparticles. *J. Mol. Liq.* **2018**, *268*, 87–101. [CrossRef]

39. Khan, S.B. Metal nanoparticles containing chitosan wrapped cellulose nanocomposites for catalytic hydrogen production and reduction of environmental pollutants. *Carbohydr. Polym.* **2020**, *242*, 116286. [CrossRef]

40. Mahmoud, M.E.; Amira, M.F.; Abouelanwar, M.E.; Seleim, S.M. Catalytic reduction of nitrophenols by a novel assembled nanocatalyst based on zerovalent copper-nanopolyaniline-nanozirconium silicate. *J. Mol. Liq.* **2020**, *299*, 112192. [CrossRef]

41. Fagieh, T.M.; Bakhsh, E.M.; Khan, S.B.; Akhtar, K.; Asiri, A.M. Alginate/banana waste beads supported metal nanoparticles for efficient water remediation. *Polymers* **2021**, *13*, 4054. [CrossRef] [PubMed]

42. Gul, S.; Khan, S.B.; Rehman, I.U.; Khan, M.A.; Khan, M.I. A comprehensive review of magnetic nanomaterials modern day theranostics. *Front. Mater. Polym. Compos. Mater.* **2019**, *6*, 179. [CrossRef]

43. Kim, D.; Jung, J.; Kim, Y.; Lee, M.; Seo, J.; Khan, S.B. Structure and thermal properties of octadecane/expanded graphite composites as shape-stabilized phase change materials. *Int. J. Heat Mass Transf.* **2016**, *95*, 735–741. [CrossRef]